https://doi.org/10.4047/jap.2022.14.5.315

Effect of barium silicate filler content on mechanical properties of resin nanoceramics for additive manufacturing

Sun Won, Kyung-Ho Ko, Chan-Jin Park, Lee-Ra Cho, Yoon-Hyuk Huh*

Department of Prosthodontics and Research Institute of Oral Science, College of Dentistry, Gangneung-Wonju National University, Gangneung, Republic of Korea

ORCID

Sun Won
https://orcid.org/0000-0003-0514-6247

Kyung-Ho Ko
https://orcid.org/0000-0002-1260-8844

Chan-Jin Park
https://orcid.org/0000-0003-4734-214X

Lee-Ra Cho
https://orcid.org/0000-0003-3989-2870

Yoon-Hyuk Huh
https://orcid.org/0000-0003-4072-5199

PURPOSE. The purpose of this study was to investigate the effect of barium silicate filler contents on mechanical properties of resin nanoceramics (RNCs) for additive manufacturing (AM). **MATERIALS AND METHODS.** Additively manufactured RNC specimens were divided into 4 groups depending on the content of ceramic fillers and polymers: 0% barium silicate and 100% polymer (B0/P10, control group); 50% barium silicate and 50% polymer (B5/P5); 60% barium silicate and 40% polymer (B6/P4); 67% barium silicate and 33% polymer (B6.7/P3.3). The compressive strength (n = 15) and fracture toughness (n = 12) of the specimens were measured, and scanning electron microscopy (SEM) with energy dispersive X-ray spectroscopy (EDS) analyses were performed. Independent sample Kruskal-Wallis tests were performed on the compressive strength and fracture toughness test results, and the significance of each group was analyzed at the 95% confidence interval through post-tests using the Bonferroni's method. **RESULTS.** B6/P4 and B6.7/P3.3 exhibited much higher yield strength than B0/P10 and B5/P5 ($P < .05$). Compared to the control group (B0/P10), the other three groups exhibited higher ultimate strength ($P < .05$). The fracture toughness of B6/P4 and B6.7/P3.3 were similar ($P > .05$). The content of barium silicate and fracture toughness showed a positive correlation coefficient (R = 0.582). SEM and EDS analyses revealed the presence of an oval-shaped ceramic aggregate in B6/P4 specimens, whereas the ceramic filler and polymer substrate were homogeneously mixed in B6.7/P3.3. **CONCLUSION.** Increasing the ceramic filler content improves the mechanical properties, but it can be accompanied by a decrease in the flowability and the homogeneity of the slurry. [J Adv Prosthodont 2022;14:315-23]

KEYWORDS

Additive manufacturing; Resin nanoceramic; Barium silicate; Fracture toughness

Corresponding author
Yoon-Hyuk Huh
Department of Prosthodontics, College of Dentistry, Gangneung-Wonju National University, 7 Jukheon-gil, Gangneung-si, Gangwon-do 25457, Republic of Korea
Tel +82 33 640 2758
E-mail vino@gwnu.ac.kr

Received May 5, 2022 /
Last Revision September 21, 2022 /
Accepted October 17, 2022

This study was supported by 2021 Academic Research Support Program in Gangneung-Wonju National University.

INTRODUCTION

Compared with computer-aided design and computer-aided milling, additive manufacturing (AM) can produce more complex shapes without requiring ex-

https://doi.org/10.4047/jap.2022.14.5.315

pensive instruments.[1-3] Stereolithography (SLA) manufacturing is one of the AM methods defined by the American Society for Testing and Materials (ASTM)[4] and is widely used in various fields to rapidly produce parts with high quality surfaces.[5,6] The SLA method uses a photopolymerizable material.[7,8] The degree of polymerization was affected by the light source, thickness of the layer, properties of the material, type of photopolymerization initiator, and the presence of other additive components.[2-8] This implies that the mechanical properties of the definitive product will vary depending on the manufacturing conditions.

Polymers are the most widely studied and used materials for SLA. They are used for manufacturing dental casts, customized trays, orthodontic devices, occlusal stabilization devices, and guides for implant surgery. However, the poor mechanical properties of polymers limit their application in dental clinics. Conversely, ceramics, which are also widely used for manufacturing prosthetics, have various advantages, such as excellent mechanical properties, esthetics, biocompatibility, and stability.[9] However, it is quite difficult to fabricate ceramic parts using AM. Post-processing of ceramics involve debinding (to remove organic substances) and sintering (to reinforce the structure).[10] This procedure requires stringent manufacturing conditions to prevent the degradation of surface quality, mechanical strength decrease (due to defects or bubbles), and volume changes of the ceramic.

Generally, the elastic modulus of ceramics is higher than that of teeth.[11-13] Mixtures of polymers and ceramics, such as polymer-infiltrated ceramic networks and resin nanoceramics (RNCs), were developed to decrease the brittleness of ceramics and increase the flexibility, fracture toughness, and machinability of the polymers.[13,14] Polymer-infiltrated ceramic networks are mainly processed through milling, while RNCs are used for AM. RNC blocks for milling have a ceramic filler content of approximately 65 - 74%.[15] The production of milling blocks with polymer-infiltrated ceramic networks is declining because their properties are poorer than expected. However, manufacturing RNCs by AM is still attractive from the viewpoint of producing the desired complex shape.

To use the RNC in AM, it is necessary to evaluate the mechanical properties of the product during the fabrication stage. The mechanical properties of RNCs are affected by both the content and distribution of ceramic fillers. While zirconia and alumina are the most commonly used ceramic fillers for AM, glass ceramics are also can be used.[1] For example, owing to their suitable mechanical properties and shape accuracy, lithium disilicate glass ceramics have been used for the SLA-based AM of dental prosthesis.[15] In addition, barium silicate, which is easily mixed with a polymer via silanization, can be successfully used in AM. However, few studies have investigated the effects of glass ceramic filler and resin monomer ratio on the mechanical properties of the additively manufactured part. In addition, it is necessary to determine the homogeneity of the slurry according to the components constituting the resin monomer.

In this study, the mechanical properties and microstructure of an RNC produced by mixing a crystallized glass filler composed of barium silicate and a resin polymer substrate for AM were evaluated and their optimal mixing ratio to produce a material suitable for dental applications was determined. The null hypothesis was that the proportion of barium silicate crystals will not affect the mechanical properties of RNCs.

MATERIALS AND METHODS

All inorganic materials, including barium silicate crystals, were pre-silanated prior to addition to the resin (Table 1). A silane coupling agent was used for surface modification of barium silica nanoparticles, 3-(Trimethoxysilyl)propyl methacrylate (TMSPMA). The materials were placed in a stirrer (SM500D; Global Lab, Siheung, Korea) and mixed at a constant speed of 150 rpm. Samples were mixed for 2 hours between 21 and 23 degrees Celsius using a vacuum pump (MVP36; Woosung Vacuum, Jeju, Korea). The components of the RNC used in this study are listed in Table 1.

Preliminary experiments were conducted to maximize the amount of ceramic filler to ensure that the RNC has favorable mechanical properties. The minimum content of 50% ceramic filler was set, and the amount of ceramic filler was increased in small steps. The control group was 0% barium silicate and 100%

Table 1. Materials used for the fabrication of the slurry for additive manufacturing (AM)

Material	Product name	Model No.	Lot No. CAS No.	Manufacturer
Inorganic filler (Ba, Ca, Al, Quartz)	Barium glass	SG-BAG700GBFCMP5	SG-ZNNCZXC5	Sukgyung AT
Inorganic filler (Silica)	Fumed silica	AEROSIL-R972	617080581	Evonik Industries
Inorganic filler (Iron oxide)	Iron (II, III) oxide	5020-4405	1317-61-9 (CAS No.)	Daejung
Monomer (Bis-GMA)	Bisphenol A glycerolate dimethacrylate	494356-100 ml	1565-94-2 (CAS No.)	Aldrich
Monomer (TEGDMA)	Triethylene glycol dimethacrylate	261548-1 L	STBH2136	Aldrich
Monomer (UDMA)	Diurethane dimethacrylate	436909-500 ml	MKCG8230	Aldrich
Silane coupling agent	3-(Trimethoxysilyl)propyl methacrylate	261548-1 L	SHBK1531	Aldrich
Photopolymerizing initiator	Camphoroquinone	124893-5 g	09003AQV	Aldrich
Photopolymerizing stabilizer	Hydroquinone	H17902-500 g	123-31-9 (CAS No.)	Aldrich

polymer. The maximum amount of ceramic filler that enabled a smooth product was 67%, and it was difficult to obtain a homogeneous product at higher ceramic fractions. The RNCs were divided into three groups depending on their proportion of inorganic fillers and polymers. The samples are henceforth referred to as Bx/Py, where B and P refer to the barium silicate and polymer, respectively, and x and y are the corresponding weight fractions. Samples B0/P10, B5/P5, B6/P4, and B6.7/P3.3 were prepared and analyzed. A Moai 200 laser SLA three-dimensional (3D) printer (Peopoly, Los Angeles, CA, USA) with dimensions of 200 mm (both X and Y directions) by 250 mm (Z direction) was used (Table 2). The specimens were printed perpendicular to the surface of the fracture test. After AM, the specimens were post-processed for 30 min using a Wash and Cure system (Anycubic, Shenzhen, China).

The mechanical properties of the manufactured RNCs were compared to those of three commercially available milling materials, namely, Real Fit (HASEM, Daegu, Korea), which is polymethyl methacrylate (PMMA), Lava Ultimate (3M ESPE, St. Paul, USA), and Leucite glass ceramic containing Rosetta BM (HASS, gangneung, Korea). The specimens for milling to the same dimensions were designed using a computer-aided design (CAD) program (SolidWorks; Dassault Systèmes, Waltham, MA, USA) and fabricated using a computer-aided manufacturing (CAM) milling machine (CORiTEC 250i; imes-icore GmbH, Eiterfeld, Germany).

Table 2. Printing parameters

Parameters	Conditions
One layer polymerizing time (s)	4 - 6
Bottom layer polymerizing time (s)	5 - 8
One layer thickness (mm)	0.02 - 0.05
Wavelength (nm)	UV LED 405
LED radiant flux (mW)	1100 - 1300

For compression tests, 15 cylindrical specimens with 6 mm diameter and 9 mm height were prepared for each group. According to a statistical power analysis using G*Power (G*Power 3.1.9.2, Heinrich-Heine University, Dusseldorf, Germany) based on the pilot study ($\alpha = 0.05$, power $(1-\beta) = 0.95$), the appropriate number of specimens for the compression test was 15 per group. The size of the specimen was designed by calculating the shrinkage according to the mixing ratio. Next, the specimen surfaces were polished. Uniaxial compression tests was performed with a universal testing machine (Model 5982 Instron; Norwood, MA, USA) having a crosshead speed of 0.5 mm/min in accordance with ASTM C1424-16. The elastic modulus and compression data (yield strength and ultimate strength) of the specimens were calculated from

https://doi.org/10.4047/jap.2022.14.5.315

stress-strain curves.

For the fracture toughness tests, the appropriate number of specimens was determined to be ~4. However, considering other variables, the number of specimens for these tests was set as 12. Twelve bar-shaped specimens with a V-notch were produced for each group (B5/P5, B6/P4, B6.7/P3.3) in accordance with ISO 20795-1.[16] Since the control group was a polymer without ceramic filler, the fracture toughness was measured only for the test group (B5/P5, B6/P4, and B6.7/P3.3). A single-edge V-notched beam (SEVNB) technique was used to measure the fracture toughness of the specimens. The tests were conducted using a universal testing machine (AGS-10kNX; Shimadzu, Kyoto, Japan) with a crosshead speed of 1.0 mm/min. The fracture toughness K_{IC} was calculated using the following formula

$$K_{IC} = \frac{4P}{B}\sqrt{\frac{\pi}{W}}\left[1.6\left(\frac{\alpha}{W}\right)^{1/2} - 2.6\left(\frac{\alpha}{W}\right)^{3/2} + 12.3\left(\frac{\alpha}{W}\right)^{5/2} - 21.2\left(\frac{\alpha}{W}\right)^{7/2} + 21.8\left(\frac{\alpha}{W}\right)^{9/2}\right],$$

where P is the applied load; B is the width of the specimen; α is the depth of the V-notch; W is the height of the specimen.

The surface of the B6/P4 and B6.7/P3.3 specimens was observed using scanning electron microscopy (SEM, FEI Quanta FEG 250; Hillsboro, OR, USA) at magnifications of 500× and 3000× and energy dispersive X-ray spectroscopy (EDS) analysis was performed to compare elemental compositions.

Statistical analysis was performed using the SPSS statistics program (IBM SPSS 23.0; IBM Corp., Armonk, NY, USA). Normality and homogeneity of variance tests of the measurements were performed through Shapiro-Wilk and Levene's tests. Because the data did not satisfy either normality or homogeneity of variance, a Kruskal-Wallis test was performed, followed by multiple Bonferroni comparisons. The statistical significance was analyzed at the 95% confidence interval.

RESULTS

Table 3 lists the yield strength, ultimate strength, and elastic modulus of the specimens. No statistically significant difference in the yield strength between the B0/P10 and B5/P5 groups was observed (P = .433). The mean yield strengths of the B6/P4 and B6.7/P3.3 groups were 106.18 ± 8.29 and 150.23 ± 13.46 MPa, respectively, which were not significantly different (P = .112). The B6/P4 and B6.7/P3.3 groups showed significantly higher yield strength values than the B0/P10 and B5/P5 groups (P < .05).

A statistically significant difference was observed between the ultimate strength values of the control group (B0/P10) and the other three test groups (P < .05) but not between B5/P5 and B6/P4 (P = 1.000), B5/P5 and B6.7/P3.3 (P = .100), or B6/P4 and B6.7/P3.3 (P = .115).

The difference in the moduli of elasticity of the B5/P5 and B6/P4 groups was not statistically significant (P = .750); these two test groups showed significantly higher moduli of elasticity than the B0/P10 group (P < .05). The B6.7/P3.3 group showed higher modulus of elasticity than the B5/P5 and B6/P4 groups (P < .05).

According to a previous study,[17] the yield strength of PMMA for CAD-CAM is 130.67 MPa and the ultimate yield strength is 289.7 MPa. The average modulus of elasticity was reported to be 2.52 GPa. Therefore, all experimental groups except B6.7/P3.3 showed lower yield strength than that of PMMA. The ultimate yield strength and modulus of elasticity measured for the test groups were higher than those of PMMA in all groups except B0/P10.

Figure 1 presents a box plot of the fracture tough-

Table 3. Results of yield strength, ultimate strength, and elastic modulus

Group		Yield strength (MPa)	Ultimate strength (MPa)	Young's modulus of elasticity (GPa)
Control	B0/P10	85.47 ± 4.71[a]	248.93 ± 58.19[a]	2.19 ± 0.26[a]
	B5/P5	83.38 ± 5.90[a]	343.49 ± 25.13[b]	3.21 ± 0.17[b]
Experimental	B6/P4	106.18 ± 8.29[b]	345.11 ± 16.83[b]	3.17 ± 0.25[b]
	B6.7/P3.3	150.23 ± 13.46[b]	378.27 ± 30.97[b]	3.99 ± 0.54[c]

Different superscript lowercase letters indicate statistically significant differences (P < .05).

ness of the samples fabricated in this study. There is a positive Pearson correlation coefficient with increasing fracture toughness as the content of barium silicate increased (R = 0.582). In addition, the B6/P4 group showed statistically significantly higher fracture toughness than the B5/P5 group ($P < .05$). However, no statistically significant difference was observed in the fracture toughness between the B6/P4 and B6.7/P3.3 groups ($P = .114$).

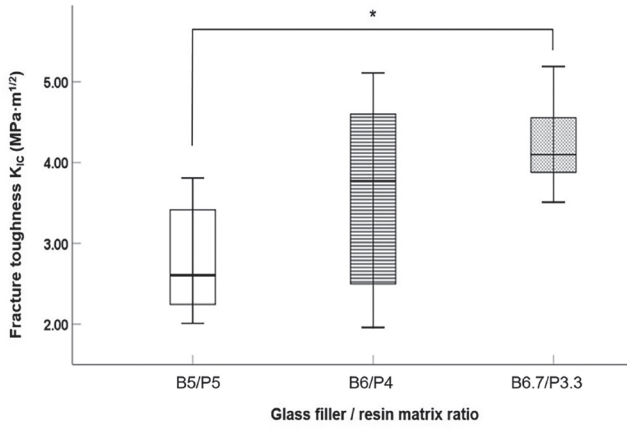

Fig. 1. Box plot of fracture toughness (K_{IC}) of experimental RNC (MPa·m$^{1/2}$).
* indicates statistically significant differences ($P < .05$).

Figure 2 exhibited SEM images of the surfaces of the B5/P5, B6/P4 and B6.7/P3.3 specimens at different magnifications.

In the B5/P5 group, elliptical ceramic crystal aggregates with a size of approximately 10 - 30 μm (Fig. 2 A, D) were observed. In the B6/P4 group, these aggregates were larger (30 - 50 μm; Fig. 2 B, E). In contrast, the microstructure of the B6.7/P3.3 group was uniform without clear distinction between the ceramic crystal aggregates and polymer substrate. The images at 500× and 3000× magnification show that the barium silicate crystals are uniformly distributed in the polymer matrix (Fig. 2 C, F).

Figure 3 presented the EDS results from the region of the elliptical ceramic crystal aggregate of the B6/P4 group observed on the SEM images and the surrounding region. A higher distribution of Si and O elements and a relatively lower distribution of C elements was observed in the crystal area (selected area 1 in Fig. 2E) than in the surrounding area (selected area 2 in Fig. 2E).

The B6.7/P3.3 group showed a uniform mixing pattern on the SEM images; thus, EDS was performed on the entire area. Figure 3C showed the EDS results from the B6.7/P3.3 specimens. The figures reveal that the B6.7/P3.3 specimen contained more Si and O and less C than the than the B6/P4 specimen.

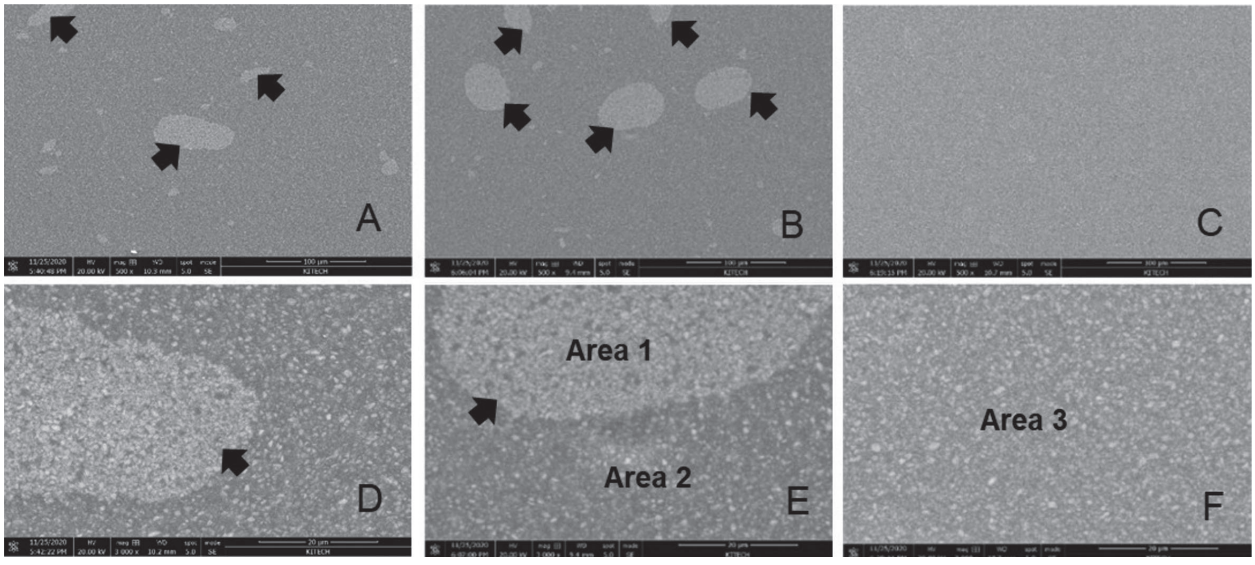

Fig. 2. SEM images of the B5/P5 (A, D), B6/P4 (B, E) and B6.7/P3.3 (C, F) specimens at magnifications ×500 and ×3,000 respectively. Black arrows indicate the region of ceramic crystal aggregation.

https://doi.org/10.4047/jap.2022.14.5.315

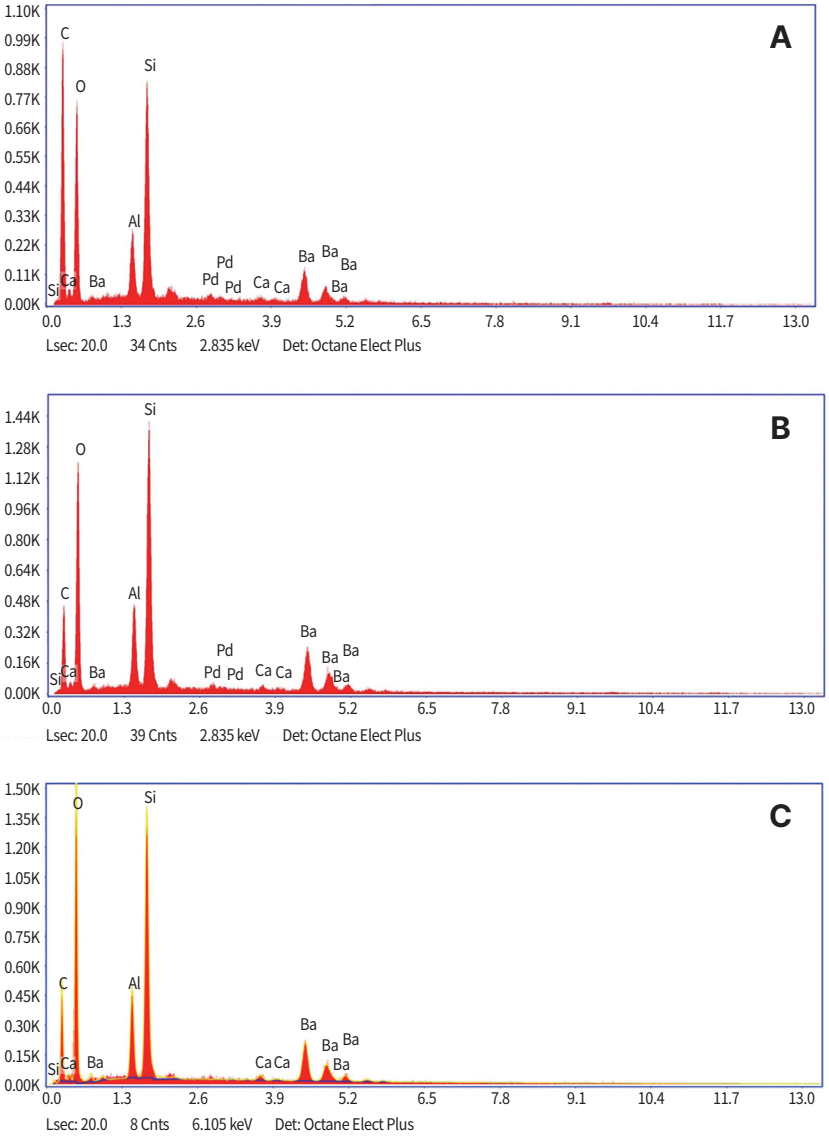

Fig. 3. Representative EDS spectra of variation elements (A) Area 1 in Figure 2E, (B) Area 2 in Figure 2E in B6/P4 specimen. (C) Area 3 in Figure 2F in B6.7/P3.3 specimen. EDS, energy-dispersive x-ray spectroscopy.

DISCUSSION

As the compressive strength, elastic modulus, and fracture toughness of the RNCs improved with an increase in the barium silicate content, the null hypothesis was rejected. The yield strength was higher when the barium silicate content was more than 50%. However, while the yield strength of B6/P4 specimens was significantly higher than those of the B0/P10 and B5/P5 specimens, it was similar to that of the B6.7/P3.3 specimens. In the case of B6.7/P3.3 specimens, a polymer substrate was formed by increasing the content of TEGDMA, a monomer with relatively low viscosity. The composition of the resin matrix was adjusted to offset the decrease in flowability of the slurry due to the increase in ceramic filler content.

Therefore, the increase in the ceramic filler content as well as state of mixing of the slurry in which the filler is homogeneously mixed with the matrix can affect the improvement in the compressive strength of the RNC. If the ceramic filler is not evenly mixed with the resin, agglomeration occurs, and the filler content

may have a weaker effect. In another pilot study, the flowability of slurry was observed to rapidly decrease when its viscosity increased above a certain level. Initially, we set the maximum ceramic filler content to 70% (rather than 67%), but the specimen could not be successfully fabricated. Baumgartner *et al*.[15] found that the viscoelastic properties of ceramic slurry had a strong relationship with its temperature. Dehurtevent *et al*.[18] showed that the viscosity of the slurry and the content of dry matter in it affected the mechanical properties of the manufactured specimens. Johansson *et al*.[19] studied the change in viscosity of the slurry with the addition of different components. However, an increase in the ceramic filler content to improve the mechanical properties can hinder the flowability.

The fracture toughness is an important mechanical property of dental restorations as it indicates the brittleness and elasticity of the material.[20] The RNCs tested showed higher fracture toughness (K_{IC} = 2.81-4.19 MPa·$m^{1/2}$) compared to those of resins measured in previous studies.[21,22] The reported elastic modulus of Lava Ultimate, a commercial RNC, is 12.77 ± 0.99 GPa.[23] However, in this study, its elastic modulus was observed to be relatively low (8.47 ± 0.99 GPa). These differences may be caused by the non-uniform shape and high surface roughness of the specimens fabricated in this study. According to Fischer *et al*.,[24] the design of the notch affects the fracture toughness. The top and bottom surfaces of the specimens should be flat and parallel to each other for an accurate compressive test. However, surfaces of the specimens produced via AM were rough, and the accuracy of the polishing process was relatively low compared to that of milling. Therefore, it is not appropriate to directly compare the relatively high fracture toughness values obtained in this study with those of previous studies. The B6/P4 and B6.7/P3.3 specimens showed higher compressive strength than PMMA. The results of this study agree with the observation that materials with a relatively low strength and elastic modulus have high fracture resistance[25] and confirm the potential of RNC for application in AM.

The fracture toughness of the B6.7/P3.3 specimens was higher than that of the B5/P5 specimens. However, the fracture toughness of B6/P4 was not significantly different from that of the B5/P5 and B6.7/P3.3 specimens. This indicates that in addition to the barium silicate content, other conditions, such as the microstructure, can affect the fracture toughness of the RNC. Kruzic *et al*.[26] proposed that depending on the composition of ceramics, microstructures resist fracture and fatigue progression through different reinforcing mechanisms. The SEM analysis results indicated that elliptical clusters of the ceramic crystal formed in the B6/P4 specimens. In this case, when the ceramic crystal and polymer substrate were separated, the cracks propagated through the latter. In contrast, the B6.7/P3.3 specimens effectively resisted the propagation of cracks because the ceramic and the polymer substrate were uniformly mixed and the number of ceramic crystals was higher. Furthermore, the fracture toughness values of the B6/P4 specimens had a large spread, and therefore, no difference with the B5/P5 specimens was observed. The reason for this result was that the mixing of the ceramic crystal and polymer substrate was not uniform. Therefore, it is necessary to develop a more suitable material condition considering not only the ratio of the filler to the polymer but also the changes in composition, viscosity, and type of additives.

As mentioned earlier, oval-shaped ceramic crystal aggregates of approximately 30 - 50 μm size were observed in the B6/P4 specimens, and their elemental composition (via EDS) was distinct from that of the rest of the region. Carbon contents in the aggregates and the rest of the region were 27% and 48%, respectively, which confirm that the dominant constituent was the polymer matrix. In contrast, Si and O, which are the constituents of the glass ceramic, were largely observed in the aggregates. Unlike in the B6/P4 specimens, the ceramic crystal and polymer substrate in the B6.7/P3.3 specimens were mixed homogeneously. Moreover, high Si and O contents and low C content were observed across the entire region in the B6.7/P3.3 than B6/P4 specimens. Although the difference in the fracture toughness between B6.7/P3.3 and B6/P4 was not statistically significant, it is believed that the low standard deviation of the B6.7/P3.3 group could be due to this uniformity.

In general, the polymerization shrinkage of a photopolymerizable resin is affected by the filler content.

https://doi.org/10.4047/jap.2022.14.5.315

When the filler content exceeds 80%, the shrinkage rate considerably decreases to approximately 0.1%.[27] In contrast, the shrinkage rate is approximately 1.5 - 1.9% when the filler content is 70 - 75%.[28] As the filler content in this study was approximately 60 - 67%, a shrinkage of approximately 2 - 3% could be expected. In addition, the polymerization shrinkage rate depends on the uniformity of the slurry. In addition to the shrinkage that occurs during the curing of RNCs, AM also results in relatively high shrinkage owing to the building procedure and post-polymerizing process and the low thickness of the layer.[29]

As a limitation of this study, it was not possible to analyze the effect of the resin matrix composition to improve the flowability, and various treatments such as the stirring method or application of a dispersant to obtain a uniform slurry were not considered. In particular, this *in vitro* study confirmed only basic mechanical properties according to AM conditions by limiting the study of the mechanical properties to basic specimen shapes. Therefore, further research on the optical properties of the composite should be investigated in the future, and additional studies on the physical properties and precision of the RNC produced by AM for samples with complex three-dimensional shapes such as real prostheses will be valuable.

CONCLUSION

Within the limitations of this *in vitro* study, the following conclusions can be drawn. Only B6.7/P3.3 group showed higher yield strength than PMMA, but ultimate yield strength and modulus were higher than PMMA in all groups except polymer B0/P10 only. The fracture toughness tends to increase as the content of the ceramic filler increases, but this may be accompanied by a decrease in the flowability and homogeneity of the slurry. Changes in the resin matrix composition can offset flow degradation, but can also affect mechanical properties. Therefore, since it is important to increase the content of ceramic fillers with guaranteed flowability and homogeneity of the slurry for AM for RNC, additional research on slurry preparation such as stirring method or dispersant application is required.

REFERENCES

1. Galante R, Figueiredo-Pina CG, Serro AP. Additive manufacturing of ceramics for dental applications: A review. Dent Mater 2019;35:825-46.
2. Hull CW. Apparatus for production of three dimensional objects by stereolithography. US-6027324-A, 2000.
3. Methani MM, Revilla-Leon M, Zandinejad A. The potential of additive manufacturing technologies and their processing parameters for the fabrication of all-ceramic crowns: A review. J Esthet Restor Dent 2020;32:182-92.
4. ASTM F2792-12A. Standard terminology for additive manufacturing technologies. West Conshohocken, PA: ASTM International; 2012.
5. Azari A, Nikzad S. The evolution of rapid prototyping in dentistry: a review. Rapid Prototyp J 2009;15:216-25.
6. Jockusch J, Özcan M. Additive manufacturing of dental polymers: An overview on processes, materials and applications. Dent Mater J 2020;39:345-54.
7. Li H, Song L, Sun J, Ma J, Shen Z. Stereolithography-fabricated zirconia dental prostheses: concerns based on clinical requirements. Adv Appl Ceram 2020;119:236-43.
8. Chartier T, Chaput C, Doreau F, Loiseau M. Stereolithography of structural complex ceramic parts. J Mater Sci 2002;37:3141-7.
9. Furtado de Mendonca A, Shahmoradi M, Gouvêa CVD, De Souza GM, Ellakwa A. Microstructural and mechanical characterization of CAD/CAM materials for monolithic dental restorations. J Prosthodont 2019;28:e587-e594.
10. Guilardi L, Soares P, Werner A, de Jager N, Pereira G, Kleverlaan C. Fatigue performance of distinct CAD/CAM dental ceramics. J Mech Behav Biomed Mater 2020;103:103540.
11. El Zhawi H, Kaizer MR, Chughtai A, Moraes RR, Zhang Y. Polymer infiltrated ceramic network structures for resistance to fatigue fracture and wear. Dent Mater 2016;32:1352-61.
12. Coldea A, Swain MV, Thiel N. Mechanical properties of polymer-infiltrated-ceramic-network materials. Dent Mater 2013;29:419-26.
13. Lauvahutanon S, Takahashi H, Shiozawa M, Iwasaki N,

Asakawa Y, Oki M, Finger WJ, Arksornnukit M. Mechanical properties of composite resin blocks for CAD/CAM. Dent Mater J 2014;33:705-10.
14. Branco AC, Silva R, Santos T, Jorge H, Rodrigues AR, Fernandes R. Suitability of 3D printed pieces of nanocrystalline zirconia for dental applications. Dent Mater 2020;36:442-55.
15. Baumgartner S, Gmeiner R, Schönherr JA, Stampfl J. Stereolithography-based additive manufacturing of lithium disilicate glass ceramic for dental applications. Mater Sci Eng C Mater Biol Appl 2020;116:111180.
16. ISO 20795-1. Dentistry-Base polymers-Part 1: Denture base polymers. 2nd ed. International Standard Organization (ISO); Geneva; Switzerland, 2013.
17. Al-Dwairi ZN, Tahboub KY, Baba NZ, Goodacre CJ. A Comparison of the flexural and impact strengths and flexural modulus of CAD/CAM and conventional heat-cured polymethyl methacrylate (PMMA). J Prosthodont 2020;29:341-9.
18. Dehurtevent M, Robberecht L, Hornez JC, Thuault A, Deveaux E, Béhin P. Stereolithography: A new method for processing dental ceramics by additive computer-aided manufacturing. Dent Mater 2017;33:477-85.
19. Johansson E, Lidstrom O, Johansson J, Lyckfeldt O, Adolfsson E. Influence of resin composition on the defect formation in alumina manufactured by stereolithography. Materials (Basel) 2017;10:138.
20. Della Bona A, Corazza PH, Zhang Y. Characterization of a polymer-infiltrated ceramic-network material. Dent Mater 2014;30:564-9.
21. Ilie N, Hickel R, Valceanu AS, Huth KC. Fracture toughness of dental restorative materials. Clin Oral Investig 2012;16:489-98.
22. Hampe R, Theelke B, Lümkemann N, Eichberger M, Stawarczyk B. Fracture toughness analysis of ceramic and resin composite CAD/CAM material. Oper Dent 2019;44:E190-201.
23. Wang H, Cui B, Li J, Li S, Lin Y, Liu D. Mechanical properties and biocompatibility of polymer infiltrated sodium aluminum silicate restorative composites. J Adv Ceram 2017;6:73-9.
24. Fischer H, Waindich A, Telle R. Influence of preparation of ceramic SEVNB specimens on fracture toughness testing results. Dent Mater 2008;24:618-22.
25. Swain MV, Coldea A, Bilkhair A, Guess PC. Interpenetrating network ceramic-resin composite dental restorative materials. Dent Mater 2016;32:34-42.
26. Kruzic JJ, Arsecularatne JA, Tanaka CB, Hoffman MJ, Cesar PF. Recent advances in understanding the fatigue and wear behavior of dental composites and ceramics. J Mech Behav Biomed Mater 2018;88:504-33.
27. Sun C, Xu D, Hou C, Zhang H, Li Y, Zhang Q, Wang H, Zhu M. Core-shell structured SiO_2@ZrO_2@SiO_2 filler for radiopacity and ultra-low shrinkage dental composite resins. J Mech Behav Biomed Mater 2021;121:104593.
28. Wang Z, Chiang MYM. System compliance dictates the effect of composite filler content on polymerization shrinkage stress. Dent Mater 2016;32:551-60.
29. Digholkar S, Madhav VN, Palaskar J. Evaluation of the flexural strength and microhardness of provisional crown and bridge materials fabricated by different methods. J Indian Prosthodont Soc 2016;16:328-34.